

# Directional bond breaking by polarization-gated two-color ultrashort laser pulses

Kang Lin, Xiaochun Gong, Qiying Song, Qinying Ji, Wenbin Zhang, Junyang Ma, Peifen Lu, Haifeng Pan, Jingxin Ding, Heping Zeng and Jian Wu

State Key Laboratory of Precision Spectroscopy, East China Normal University, Shanghai 200062, People's Republic of China

E-mail: [jwu@phy.ecnu.edu.cn](mailto:jwu@phy.ecnu.edu.cn)

Received 21 August 2015, revised 5 November 2015

Accepted for publication 23 November 2015

Published 21 December 2015



CrossMark

## Abstract

We experimentally investigate directional bond breaking in dissociative single ionization of  $H_2$  driven by circularly polarized two-color ultrashort pulses of counter- and co-rotating laser fields. Trefoil or semilunar patterns of directional proton emission in a two-dimensional space spanned by the laser fields are observed, which can be finely controlled by varying the relative phase of the counter- or co-rotating circularly polarized two-color fields, respectively. Our results open new possibilities to manipulate two-dimensional directional bond breaking of molecules by strong laser fields.

Online supplementary data available from [stacks.iop.org/JPB/49/025603/mmedia](http://stacks.iop.org/JPB/49/025603/mmedia)

Keywords: strong field ionization, femtosecond laser pulse, molecular dynamics

(Some figures may appear in colour only in the online journal)

Driven by strong laser fields, electrons in a molecule can be steered to localize at one of the nuclei when the bonds break. This serves as a primary step for control of molecular reactions and has attracted much attention in the past [1–3]. Governed by the laser phase at the instant of ionization [4], the ultrashort laser pulses of asymmetric fields, e.g. carrier-envelope-phase stabilized few-cycle pulses [5–11] or two-color femtosecond pulses [12–22], are efficient tools for controlling directional bond breaking following strong-field ionization. Such control can also be achieved using a time-delayed near-infrared femtosecond pulse following the ultrafast ionization of an extreme-ultraviolet attosecond pulse [23–26]. However, these directional bond breaking controls were mostly limited to one dimension along the polarization of the laser field [4–20, 22–26]. Recently, we demonstrated that two-dimensional control of molecular bond breaking can be realized using an orthogonally polarized two-color femtosecond pulse [21], where the direction of the bond breaking is determined by the numbers of photons absorbed from the laser fields of different colors.

In this paper, for the dissociative single ionization of  $H_2$  driven by circularly polarized two-color pulses of counter- or

co-rotating laser fields, we observe two-dimensional trefoil or semilunar patterns of directional proton emission in the polarization plane. By varying the relative phase of the polarization-gated two-color (PTC) pulse, the trefoil or semilunar patterns can be finely controlled.

The PTC pulse created by two circularly polarized laser pulses of different frequencies can be expressed as [27]:

$$\begin{aligned} \mathbf{E}(t) = & E_1(t) [\sin(\omega_1 t) \mathbf{e}_y + \cos(\omega_1 t) \mathbf{e}_z] \\ & + E_2(t) [\pm \sin(\omega_2 t + \phi_L) \mathbf{e}_y \\ & + \cos(\omega_2 t + \phi_L) \mathbf{e}_z] \end{aligned}$$

where  $E_i(t) = E_{i0} \exp(-t^2/\tau_i^2)$  ( $i = 1, 2$ ),  $\tau_i$ ,  $E_{i0}$ , and  $\omega_i$  are the envelope, temporal duration, amplitude, and carrier frequency of the circularly polarized laser pulses,  $\phi_L$  is the relative phase between the fields of different frequencies, and  $\mathbf{e}_y$  and  $\mathbf{e}_z$  are the unit vectors along the  $y$  and  $z$  axes. The sign  $+/-$  accounts for the circularly polarized pulses of same or opposite helicities, respectively. As illustrated in figure 1(a), the laser field of the PTC pulse consisting of the fundamental wave (FW) at  $\omega_1$  and its second harmonic (SH) at  $\omega_2 = 2\omega_1$

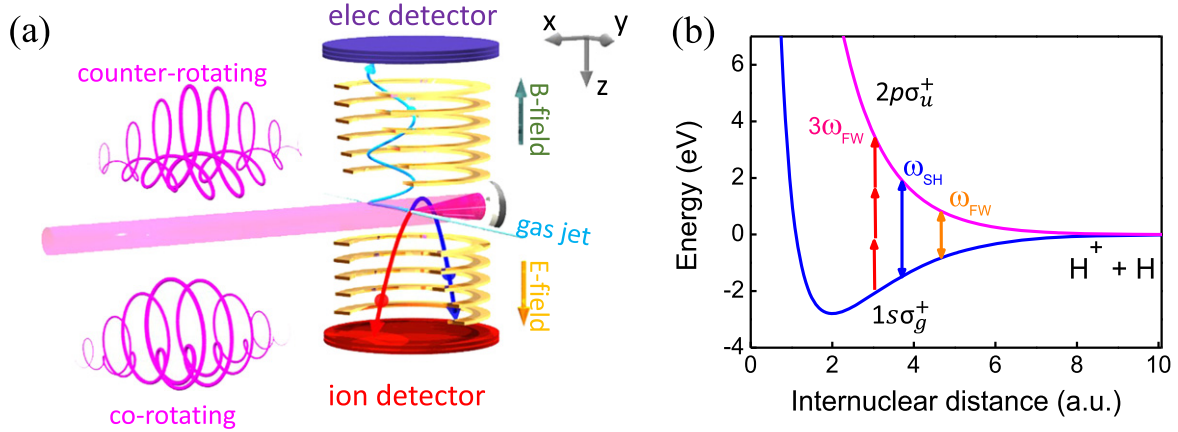


**Figure 1.** (a) Experimental setup. (b) Schematic diagram of the involved potential energy surfaces and dissociation pathways of  $\text{H}_2^+$  in the two-color fields.

of the same or opposite helicities is featured with one or three maxima in one oscillating cycle of the FW, respectively. The two-color trefoil laser field has been investigated to multidirectionally orient molecules [27], to produce circularly polarized extreme ultraviolet light [28], and to probe two-dimensional electron trajectories in order to separate the rescattered and directly freed electrons [29]. Here, based on the interference of the dissociating nuclear wave packets of opposite parities [30–34], we demonstrate that the PTC pulse can be used to two-dimensionally steer the directional bond breaking in strong-field single ionization of  $\text{H}_2$ .

Experimentally, a linearly polarized femtosecond laser pulse (25 fs, 790 nm, 10 kHz, Femtolasers) produced from a multipass amplifier Ti:sapphire laser system is down-collimated into a 150  $\mu\text{m}$ -thick  $\beta$ -barium borate ( $\beta$ -BBO) crystal to generate an SH pulse at 395 nm. The FW and SH pulses are separated by a dichroic mirror after the  $\beta$ -BBO crystal, then adjusted to produce circular polarization of the same or opposite helicities using two individual quarter wave plates in each arm. The circularly polarized FW and SH pulses are then collinearly recombined using another dichroic mirror. A motorized delay stage in one of the arms is used to temporally synchronize the FW and SH pulses. To finely tune the phase  $\phi_L$  of the PTC pulse and meanwhile overcome the ineluctable fluctuation of the relative optical path length between the FW and SH arms due to air flow or mechanical vibration, a phase-locking system based on the spatial interference of a reference continuum-wave (CW) laser at 532 nm is employed [35, 36]. To do that, the CW laser is coupled into the FW and SH arms and afterwards recombined via the same splitting and recombination mirrors for the FW and SH pulses to ensure the same optical pathways. The interference fringes of the CW laser after the recombination mirror are imaged by a CCD camera. The drift of the relative path length is extracted from the swing of the interference fringes, which is afterwards compensated by a piezo-based delay stage in the FW arm using a feedback loop. The relative phase  $\phi_L$  of the PTC pulse is tuned in the same manner by finely moving the interference fringes using the piezo-based delay stage. As schematically illustrated in figure 1(a), the PTC pulse polarized in the  $y$ - $z$  plane is then focused onto a supersonic molecular beam of  $\text{H}_2$

in an ultrahigh vacuum chamber of COLTRIMS (‘cold target recoil ion momentum spectroscopy’) [37, 38] by a concave silver mirror ( $f = 7.5$  cm). The intensities of the FW and SH pulses in the reaction region are measured to be  $I_{FW} \sim 2.8 \times 10^{14}$  and  $I_{SH} \sim 0.9 \times 10^{14} \text{ W cm}^{-2}$ , respectively. The temporal duration of the PTC pulse in the interaction region is estimated to be  $\sim 80$  fs by tracing the time-delay-dependent single ionization yield as a cross-correlation of the FW and SH pulses. The PTC pulse photoionizes  $\text{H}_2$  to  $\text{H}_2^+$  by releasing one electron in the first step. The  $\text{H}_2^+$  then dissociates into  $\text{H}^+ + \text{H}$  in the second step, hereafter labeled as the  $\text{H}_2(1,0)$  channel. The ions and electrons produced are accelerated and guided by a weak homogeneous static electric field ( $\sim 8.5 \text{ V cm}^{-1}$ ) and magnetic field ( $\sim 9$  gauss) to be detected by two time- and position-sensitive microchannel plate detectors [39] at opposite ends of the spectrometer. The three-dimensional momenta of the ions and electrons are retrieved from the measured time of flight and positions of the impacts. Since the PTC pulse is polarized in the  $y$ - $z$  plane, in the following we restrict the discussion of the two-dimensional directional bond breaking in the  $y$ - $z$  plane.

The directional bond breaking in the dissociative single ionization of  $\text{H}_2$  is investigated by observing asymmetric emission of  $\text{H}^+$  in producing the  $\text{H}_2(1,0)$  channel. To qualify the asymmetric emission of  $\text{H}^+$  in the polarization plane, we define the asymmetry parameter  $A(p_y, p_z, \phi_L) = [N(p_y, p_z, \phi_L) - N(p_y, p_z, \phi_L + \pi)] / [N(p_y, p_z, \phi_L) + N(p_y, p_z, \phi_L + \pi)]$ , where  $N(p_y, p_z, \phi_L)$  is the measured  $\text{H}^+$  yield at momentum  $\mathbf{p} = (p_y, p_z)$  and the relative phase  $\phi_L$  of the PTC pulse. The asymmetry parameter is positive if  $\text{H}^+$  is preferred to emit to  $\phi_{\text{H}^+} = \tan^{-1}(p_z/p_y)$  and negative if  $\text{H}^+$  is preferred to emit to  $\phi_{\text{H}^+} + \pi$  at  $\phi_L$ . Figure 2(a) displays the measured asymmetry of  $\text{H}^+$  ejected in the  $(p_y, p_z)$  plane at  $\phi_L = 0$  for a PTC pulse of counter-rotating laser fields. To determine the absolute phase of the PTC pulse, the momentum distribution of the freed electron is measured in coincidence with the ejected ion. Due to the angular streaking of the PTC pulse, as displayed in figure 3, the freed electron shows a momentum asymmetric pattern similar to the profile of the driving laser field [29], as illustrated in figures 3(a) and (d) for the counter- and co-rotating two-color laser fields at  $\phi_L = 0$ . Here the

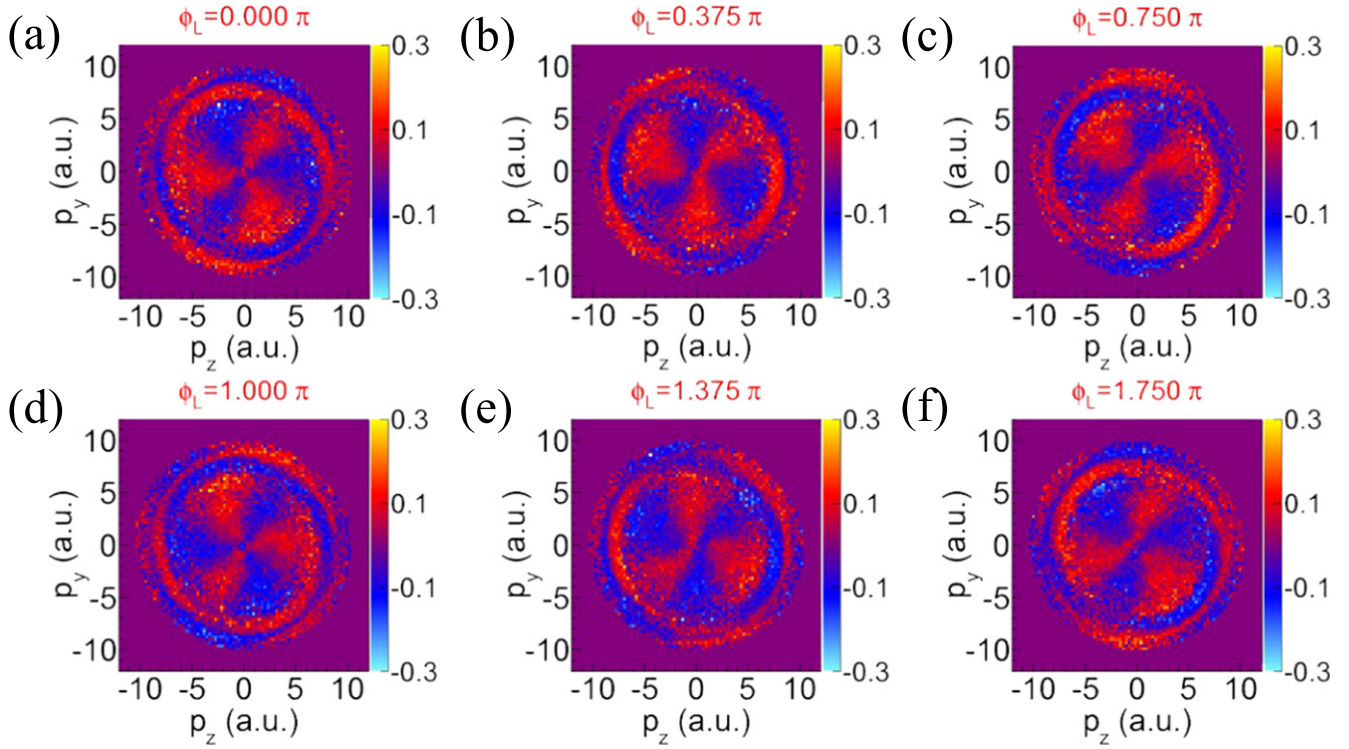


**Figure 2.** Measured two-dimensional asymmetry patterns of the directional emission of  $H^+$  in  $(p_y, p_z)$  space at different phases  $\phi_L$  of a counter-rotating PTC pulse.

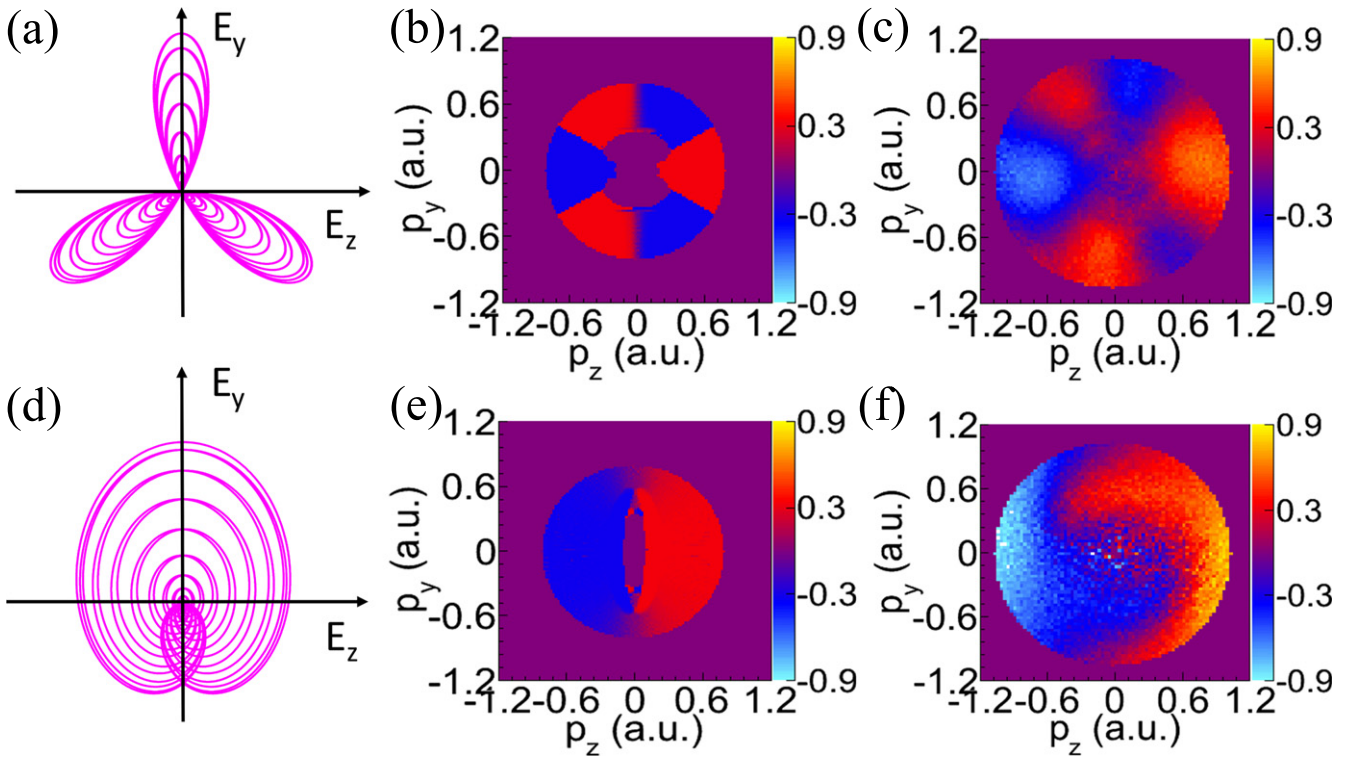


**Figure 3.** Electric fields of the (a) counter- and (d) co-rotating PTC pulses at  $\phi_L = 0$ , and the corresponding (b), (e) numerically simulated and (c), (f) experimentally measured asymmetric patterns of the freed electron in the polarization ( $y$ - $z$ ) plane.

laser phase  $\phi_L = 0$  is defined when one of the three lobes of the trefoil laser field or the maximum of the semilunar laser field orients along the  $y$ -axis. By merely considering the streaking effect of the rotating laser field, it can be seen that the freed electron released with an initial lateral velocity perpendicular to the laser vector at the ionization instant ends with a momentum pattern similar to the laser field but rotated by  $90^\circ$ . The simulated asymmetric emission of freed electrons for counter- and co-rotating PTC pulses in figures 3(b) and (e) agree very well with the experiment, as shown in figures 3(c) and (f) respectively. We thus can deduce the absolute phase of the PTC pulse by measuring the momentum distribution of the freed electron, for instance at  $\phi_L = 0$  as displayed in figures 3(c) and (f). The asymmetric emission of  $H^+$  shows a trefoil distribution for the inner part and a spiral shape for the outer part, resulting from two-dimensional interference of different dissociation pathways, as will be discussed later on. As shown in figures 2(a) and 3(a), we note that the orientation of the trefoil pattern of the asymmetric emission of  $H^+$  differs from the orientation of the laser field. This indicates the important role of the laser-phase-dependent interference of the dissociating nuclear wave packet, where the ejection direction of the proton is governed by the number of absorbed photons of different colors and does not necessarily coincide with the electric field of the largest asymmetry [21]. The asymmetry pattern rotates like a fan when the laser phase  $\phi_L$  is continuously varied (see the animated movie in the supplementary material<sup>1</sup>). Figures 2(b) to (f) display snapshots of the two-dimensional patterns of the asymmetry at different laser phases. The asymmetry pattern rotates by  $180^\circ$  when the laser phase  $\phi_L$  is increased by  $\pi$ . We therefore can control the asymmetric emission of  $H^+$  in the polarization plane on an attosecond timescale by finely adjusting the relative phase  $\phi_L$  of the PTC pulse.

The different  $\phi_L$ -dependent distributions of the asymmetry of the inner and outer parts in the  $(p_y, p_z)$  space is clearly revealed in figure 4 for instance for  $30^\circ < \phi_H^+ < 50^\circ$ , where the asymmetry is calculated as a function of the kinetic energy of  $H^+$ , i.e.  $E_H^+$ , and the laser phase  $\phi_L$ . The left panel of figure 4 shows the measured yield of  $H^+$  versus  $E_H^+$ , where the events with  $E_H^+$  greater or less than 0.6 eV are produced via different dissociation pathways. For the dipole-allowed photon transitions between the  $1s\sigma_g^+$  and  $2p\sigma_u^+$  states of  $H_2^+$ , the laser field component along the molecular axis plays an important role when it dissociates into the  $H_2(1,0)$  channel [4, 40].

In the following, we would like to understand the observed asymmetric emission of  $H^+$  of the  $H_2(1,0)$  channel using the basic picture of the dipole-allowed photon transitions governed by laser field components parallel to the molecular axis. The involved potential energy curves and dissociation pathways of the single ionized  $H_2^+$  in the two-color laser fields are illustrated in figure 1(b) [21]. The two-dimensional asymmetric emission of  $H^+$  requires the

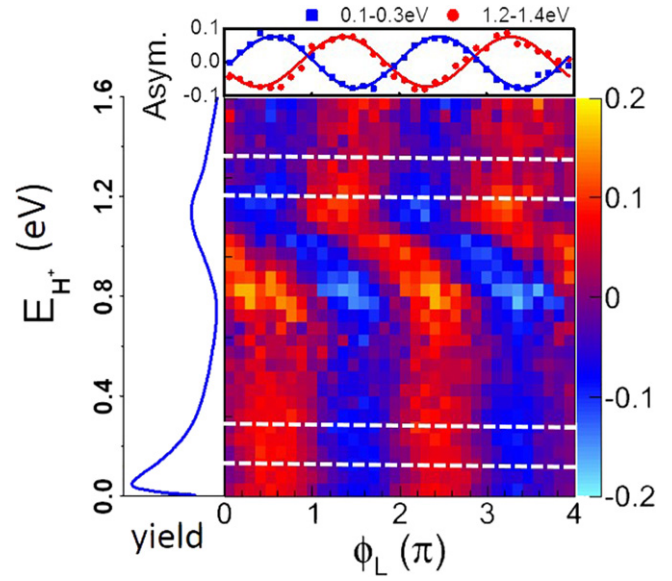


**Figure 4.** Measured asymmetries as functions of the relative phase  $\phi_L$  of a counter-rotating PTC pulse and the kinetic energy  $E_H^+$  of  $H^+$  emitted to  $30^\circ < \phi_H^+ < 50^\circ$ . The left panel is the  $E_H^+$ -dependent yield of  $H^+$ . The top panel shows the asymmetry of the directional emission of  $H^+$  versus  $\phi_L$  at low  $E_H^+$  ( $0.1 \text{ eV} < E_H^+ < 0.3 \text{ eV}$ ) and high  $E_H^+$  ( $1.2 \text{ eV} < E_H^+ < 1.4 \text{ eV}$ ) as indicated between the white dashed lines. The solid curves are the numerical fits of the measured data.

superposition of nuclear wave packets with the same kinetic energies but opposite parities dissociating along the  $1s\sigma_g^+$  and  $2p\sigma_u^+$  potential surfaces [4–26]. The superposition of the  $1\omega_{SH}-1\omega_{FW}$  pathway (propagation on the  $1s\sigma_g^+$  surface transits to the  $2p\sigma_u^+$  surface by absorbing one  $\omega_{SH}$  photon, followed by propagation on the  $2p\sigma_u^+$  curve and coupling back to the  $1s\sigma_g^+$  surface by emitting one  $\omega_{FW}$  photon, followed by dissociation along the  $1s\sigma_g^+$  surface) and the  $1\omega_{FW}$  pathway (propagation on the  $1s\sigma_g^+$  surface undergoes one- $\omega_{FW}$ -photon transition to the  $2p\sigma_u^+$  surface, followed by dissociation along the  $2p\sigma_u^+$  surface) accounts for the directional emission of  $H^+$  at  $E_H^+ < 0.6 \text{ eV}$ . In contrast, the superposition of the net- $2\omega_{FW}$  pathway (propagation on the  $1s\sigma_g^+$  surface undergoes three- $\omega_{FW}$ -photon transition to the  $2p\sigma_u^+$  surface, followed by propagation on the  $2p\sigma_u^+$  surface and then coupling back to the  $1s\sigma_g^+$  surface by emitting one  $\omega_{FW}$  photon, followed by dissociation along the  $1s\sigma_g^+$  surface) and the  $1\omega_{SH}$  pathway (propagation on the  $1s\sigma_g^+$  surface undergoes one- $\omega_{SH}$ -photon transition to the  $2p\sigma_u^+$  surface, followed by dissociation along the  $2p\sigma_u^+$  surface) leads to the directional emission of  $H^+$  at  $E_H^+ > 0.6 \text{ eV}$ . For instance, the top panel of figure 4 plots the measured asymmetry of the  $H^+$  emission versus  $\phi_L$  integrated over  $E_H^+$  intervals of 0.1–0.3 eV (low- $E_H^+$ ), and 1.2–1.4 eV (high- $E_H^+$ ), respectively, fitted by  $A = A_0 \sin(\phi_L + \phi_{A0})$  where  $A_0$  and  $\phi_{A0}$  are the amplitude and phase of the asymmetry parameter. Depending on the phase of the laser fields at the dipole-allowed transitions, the asymmetries of the directionally emitted  $H^+$  at high- and low- $E_H^+$  are almost out of

<sup>1</sup> See supplemental material for the movies of the measured two-dimensional asymmetry patterns of the directional bond breaking as a function of the phase of the counter- and co-rotating PTC pulses.

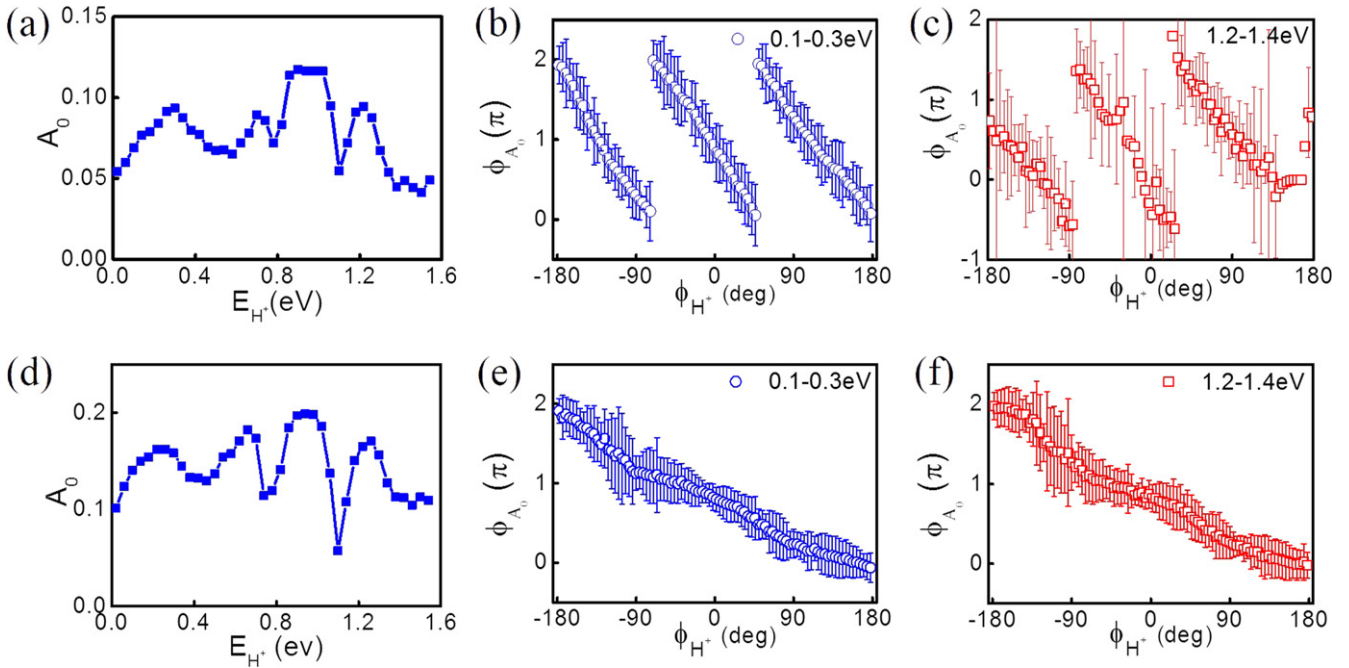


**Figure 5.** (a), (d)  $E_H^+$ -dependent amplitude  $A_0$  of the measured asymmetry integrated over  $\phi_H^+$ . (b), (c), (e), (f)  $\phi_H^+$ -dependent phase  $\phi_{A0}$  of the measured asymmetry at (b), (e) low  $E_H^+$ , and (c), (f) high  $E_H^+$ , respectively. PTC pulses of (a)–(c) counter- and (d)–(f) co-rotating laser fields are used to drive the dissociative single ionization of  $H_2$ .

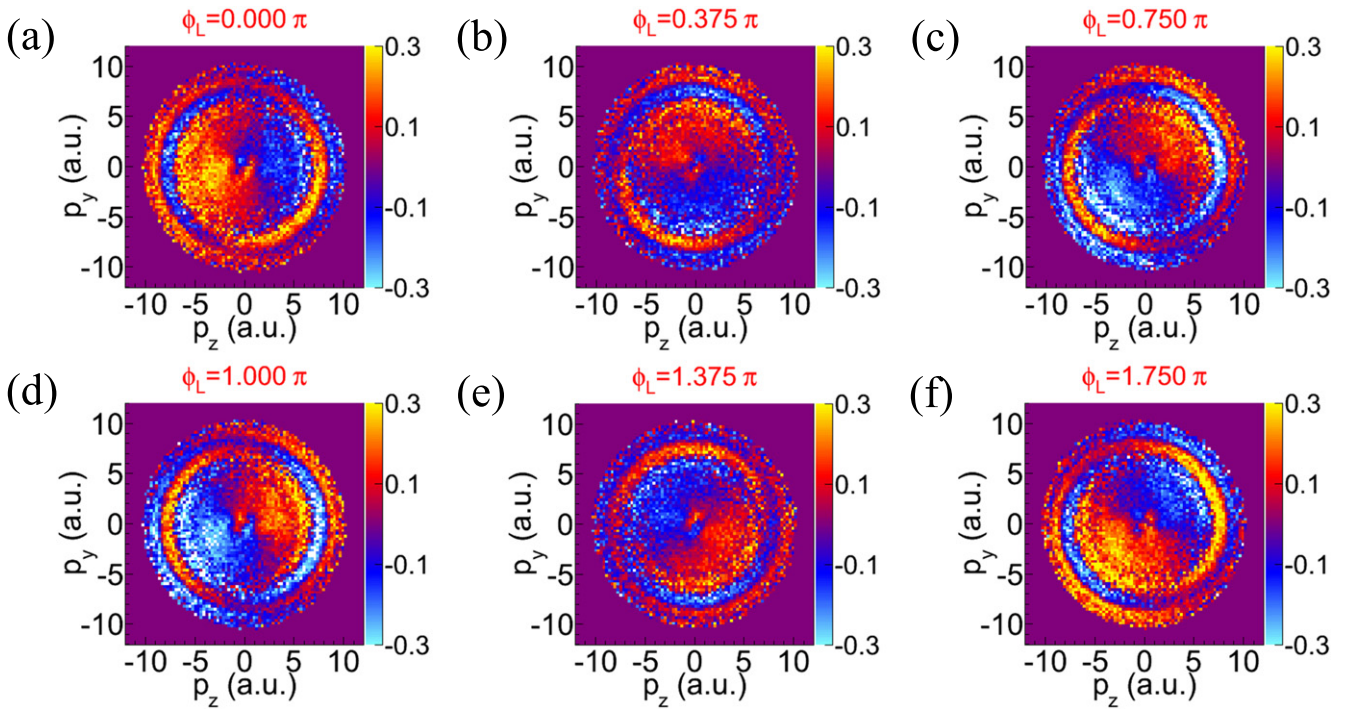


**Figure 6.** Same as figure 2 but driven by a co-rotating PTC pulse.

phase for the counter-rotating PTC pulse. The amplitude  $A_0$  of the asymmetry parameter changes as a function of  $E_H^+$  [see figure 5(a)], while the phase  $\phi_{A0}$  varies continuously as a function of  $\phi_H^+$  [see figures 5(b) and (c)]. Similar to the trefoil laser field, which has three maxima per cycle, the phase  $\phi_{A0}$  at the low- and high- $E_H^+$  regions changes by  $6\pi$  when  $\phi_H^+$  increases from  $-180^\circ$  to  $180^\circ$ .

As compared to the trefoil laser fields, as illustrated in figure 1(a), the co-rotating PTC pulse created by circularly polarized two-color pulses of the same helicity experiences one field maximum per cycle. Correspondingly, as shown in figure 6, the asymmetry of  $H^+$  ejected in  $(p_y, p_z)$  space exhibits a semilunar pattern for the inner part and a spiral shape for the outer part, respectively. The two-dimensional

asymmetry pattern rotates in the  $(p_y, p_z)$  space when the phase  $\phi_L$  of the co-rotating PTC pulse increases continuously (see the animated movie in the supplementary material<sup>1</sup>). As shown in figures 5(d) to (f), the amplitude  $A_0$  and phase  $\phi_{A0}$  of the asymmetry parameter depend on the kinetic energy  $E_{H^+}$  and the emission direction  $\phi_{H^+}$  of the ejected  $H^+$ . The phase of the asymmetry parameter changes by  $2\pi$  when  $\phi_{H^+}$  increases from  $-180^\circ$  to  $180^\circ$ , in agreement with the profile of the co-rotating PTC pulse, i.e. one field maximum per cycle. Although the FW and SH pulses used to create the PTC pulse have the same field intensities, the amplitude of the measured asymmetry using the co-rotating fields is overall larger than the counter-rotating fields.

In summary, using phase-controlled PTC pulses of counter- and co-rotating laser fields, we demonstrate that the emission direction of  $H^+$  in the dissociative single ionization of  $H_2$  can be controlled in the two-dimensional space spanned by the laser fields. Trefoil or semilunar patterns of the directional  $H^+$  emission are observed for the counter- or co-rotating PTC pulses, respectively. The two-dimensional interference of the nuclear wave packets of opposite parities allows us to manipulate the directional bond breaking in a two-dimensional space by finely tuning the relative phase of the PTC pulse.

## Acknowledgments

We thank F He and S Cui for the fruitful discussions, and Z Chang, X Wang, Q Zhang, and K Zhao for their help on the phase-locking system. This work is supported by the National Natural Science Fund (grant nos. 11425416 and 11374103), the ‘Eastern Scholar’ program, and the NCET in University (NCET-12-0177).

## References

- [1] Zewail A H 1988 *Science* **242** 1645
- [2] Assion A, Baumert T, Bergt M, Brixner T, Kiefer B, Seyfried V, Strehle M and Gerber G 1998 *Science* **282** 919
- [3] Shapiro M and Brumer P 2012 *Quantum Control of Molecular Processes* (New York: Wiley)
- [4] Wu J *et al* 2013 *Nat. Commun.* **4** 2177
- [5] Kling M F *et al* 2006 *Science* **312** 246
- [6] Kremer M *et al* 2009 *Phys. Rev. Lett.* **103** 213003
- [7] Fischer B, Kremer M, Pfeifer T, Feuerstein B, Sharma V, Thumm U, Schröter C D, Moshhammer R and Ullrich J 2010 *Phys. Rev. Lett.* **105** 223001
- [8] McKenna J, Anis F, Sayler A M, Gaire B, Johnson N G, Parke E, Carnes K D, Esry B D and Ben-Itzhak I 2012 *Phys. Rev. A* **85** 023405
- [9] Xu H, Xu T Y, He F, Kielpinski D, Sang R T and Litvinyuk I V 2014 *Phys. Rev. A* **89** 041403 (R)
- [10] Rathje T, Sayler A M, Zeng S, Wustelt P, Figger H, Esry B D and Paulus G G 2013 *Phys. Rev. Lett.* **111** 093002
- [11] Kling N G *et al* 2013 *Phys. Rev. Lett.* **111** 163004
- [12] Charron E, Giusti-Suzor A and Mies F H 1993 *Phys. Rev. Lett.* **71** 692
- [13] Ohmura H, Saito N and Tachiya M 2006 *Phys. Rev. Lett.* **96** 173001
- [14] Wu J, Vredenberg A, Schmidt L P H, Jahnke T, Czasch A and Dörner R 2013 *Phys. Rev. A* **87** 023406
- [15] Sheehy B, Walker B and DiMauro L F 1995 *Phys. Rev. Lett.* **74** 4799
- [16] Ray D *et al* 2009 *Phys. Rev. Lett.* **103** 223201
- [17] Betsch K J, Pinkham D W and Jones R R 2010 *Phys. Rev. Lett.* **105** 223002
- [18] Kotsina N, Kaziannis S, Danakas S and Kosmidisa C 2013 *J. Chem. Phys.* **139** 104313
- [19] Kaziannis S, Kotsina N and Kosmidis C 2014 *J. Chem. Phys.* **141** 104319
- [20] Ohmura H and Saito N 2014 *J. Phys. B: At. Mol. Opt. Phys.* **47** 204007
- [21] Gong X C, He P L, Song Q Y, Ji Q Y, Pan H F, Ding J X, He F, Zeng H P and Wu J 2014 *Phys. Rev. Lett.* **113** 203001
- [22] Song Q Y, Gong X C, Ji Q Y, Lin K, Pan H F, Ding J X, Zeng H P and Wu J 2015 *J. Phys. B: At. Mol. Opt. Phys.* **48** 094007
- [23] He F, Ruiz C and Becker A 2007 *Phys. Rev. Lett.* **99** 083002
- [24] He F, Ruiz C and Becker A 2008 *J. Phys. B: At. Mol. Opt. Phys.* **41** 081003
- [25] Singh K P *et al* 2010 *Phys. Rev. Lett.* **104** 023001
- [26] Sansone G *et al* 2010 *Nature* **465** 763
- [27] Chen C, Wu J and Zeng H P 2010 *Phys. Rev. A* **82** 033409
- [28] Kfir O *et al* 2015 *Nat. Photonics* **9** 99
- [29] Mancuso C A *et al* 2015 *Phys. Rev. A* **91** 031402
- [30] Tong X M and Lin C D 2007 *Phys. Rev. Lett.* **98** 123002
- [31] Roudnev V and Esry B D 2007 *Phys. Rev. Lett.* **99** 220406
- [32] Hua J J and Esry B D 2009 *J. Phys. B: At. Mol. Opt. Phys.* **42** 085601
- [33] Kelkensberg F, Sansone G, Ivanov M Y and Vrakking M 2011 *Phys. Chem. Chem. Phys.* **13** 8647
- [34] Bandrauk A D, Chelkowski S and Nguyen H S 2004 *Int. J. Quantum Chem.* **100** 834
- [35] Mashiko H, Gilbertson S, Li C Q, Khan S D, Shakya M M, Moon E and Chang Z 2008 *Phys. Rev. Lett.* **100** 103906
- [36] Chini M, Mashiko H, Wang H, Chen S, Yun C, Scott S, Gilbertson S and Chang Z 2009 *Opt. Express* **17** 21459
- [37] Dörner R, Mergel V, Jagutzki O, Spielberger L, Ullrich J, Moshhammer R and Schmidt-Böcking H 2000 *Phys. Rep.* **330** 95
- [38] Ullrich J, Moshhammer R, Dorn A, Dörner R, Schmidt L P H and Schmidt-Böcking H 2003 *Rep. Prog. Phys.* **66** 1463
- [39] Jagutzki O *et al* 2002 *IEEE Trans. Nucl. Sci.* **49** 2477
- [40] You X Y and He F 2014 *Phys. Rev. A* **89** 063405